catalysts

MDPI

Article

Recyclable Ni-Containing Coordination Polymer as an Efficient Catalyst for the Synthesis of Oxindole and Quinoline Derivatives through the Borrowing Hydrogen Strategy

Jiahao Li [1,†], Jiajie Tang [1,†], Likui Wang [1], Dawei Wang [1,*] and Zheng-Chao Duan [1,2,*]

[1] The Key Laboratory of Synthetic and Biological Colloids, Ministry of Education, School of Chemical and Material Engineering, Jiangnan University, Wuxi 214122, China; 7220610019@stu.jiangnan.edu.cn (J.L.); 1051200221@stu.jiangnan.edu.cn (J.T.); lkwang@jiangnan.edu.cn (L.W.)
[2] School of Chemical and Environmental Engineering, Hubei Minzu University, Enshi 445000, China
* Correspondence: wangdw@jiangnan.edu.cn (D.W.); 1997015@hbmzu.edu.cn (Z.-C.D.)
† These authors contributed equally to this work.

Abstract: A coordination polymer Ni-CIA has been designed, synthesized, and characterized via Fourier transform infrared spectroscopy (FT-IR), powder X-ray diffraction (XRD), scanning electron microscopy (SEM), X-ray photoelectron spectrometry (XPS), energy-dispersive X-ray spectroscopy (EDS), and thermal gravimetric analysis (TGA). The resulting polymer reveals a slice layer stacked combination structure and good stability. Importantly, this polymer exhibited high catalytic activity for the synthesis of oxindole and quinoline derivatives via borrowing hydrogen and dehydrogenation reactions. Meanwhile, several control reactions were carried out to investigate the possible mechanisms of this transformation. Finally, the results of the recycling experiment indicate that the coordination polymer Ni-CIA could be recovered and reused at least five times.

Keywords: borrowing hydrogen; dehydrogenation; annulation reactions; oxindole derivatives; quinoline derivatives

Citation: Li, J.; Tang, J.; Wang, L.; Wang, D.; Duan, Z.-C. Recyclable Ni-Containing Coordination Polymer as an Efficient Catalyst for the Synthesis of Oxindole and Quinoline Derivatives through the Borrowing Hydrogen Strategy. *Catalysts* **2023**, *13*, 1195. https://doi.org/10.3390/catal13081195

Academic Editor: Ken-ichi Fujita

Received: 3 July 2023
Revised: 27 July 2023
Accepted: 4 August 2023
Published: 9 August 2023

1. Introduction

Oxindole derivatives are privileged heterocyclic cores, constituting an important skeleton in several compounds of pharmaceutical interest with significant biological activities (Scheme 1) [1–8]. The conventional approaches for the alkylation of oxindoles employed toxic alkyl halides, suffered from harsh reaction conditions, and exhibited poor regioselectivity alongside the generation of undesired side products [9,10]. Therefore, the design and synthesis of a new catalytic system for the alkylation of oxindole derivatives has become a research hotspot in the field of organic synthesis [11–16].

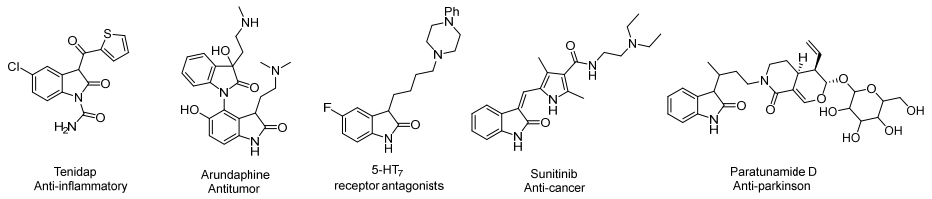

Scheme 1. Examples of biologically active C3-substituted oxindoles.

The borrowing hydrogen (BH) reaction, also known as the hydrogen autotransfer reaction, employs inexpensive alcohols as alkylation agents, generating water as the sole byproduct [17–24]. Thus, it is an atom-efficient and much greener process for the alkylation of oxindole and indole derivatives via borrowing hydrogen reactions [25–31]. In 2002, Simig and co-workers first reported that Raney nickel catalyzed the synthesis of 3-alkyloxindoles by means of the dehydrogenative coupling of 2-oxindole and alcohol

in moderate yields [32]. Later, the alkylation of oxindole with homogeneous Ru, Ir, Fe, Mn catalysts were also reported [33–37]. In 2018, we developed homogeneous pyridyl triazole-ligated ruthenium(II) complexes which could realize the selective alkylation of 2-oxindole with a variety of primary alcohols via the hydrogen autotransfer process [38]. However, homogeneous catalysts are known to have some disadvantages, such as difficulty in separation from the reaction system and their poor recyclability, which limits their further application [39–43].

Coordination polymers (CPs) have some superior properties, such as their unique channels, good stability, and effective control of their structure and functionality [44–46]. CPs have bright future applications in many fields, such as gas adsorption and separation, catalysis, and functional materials [47–49]. Organic ligands play a significant role in the design and synthesis of CPs. Recently, we reported a number of nitrogen-containing polycarboxylic acid ligands, which bind with several metal centers into chains to form CPs. Meanwhile, these CPs could be applied to some borrowing hydrogen and dehydrogenation reactions successfully [50–53]. Herein, an indolyl dicarboxylic acid ligand was used to synthesize a new Ni-containing coordination polymer, Ni-CIA (Ni-indolyl dicarboxylic acid coordination polymer), which showed excellent catalytic activity in the synthesis of oxindole and quinoline derivatives through the borrowing hydrogen strategy.

2. Results and Discussion

2.1. Characterization of Ni-CIA

After synthesis, Ni-CIA was characterized using Fourier transform infrared spectroscopy (FT-IR), powder X-ray diffraction (XRD), scanning electron microscopy (SEM), X-ray photoelectron spectrometry (XPS), energy-dispersive X-ray spectroscopy (EDS), and thermal gravimetric analysis (TGA).

The FT-IR spectra of the H_2CIA (indolyl dicarboxylic acid ligand) and Ni-CIA are shown in Figure 1a. In the spectra of H_2CIA and Ni-CIA, the characteristic absorption band at 2800~3500 cm^{-1} is attributed to O–H skeleton stretching vibrations of the hydroxyl groups. The strong absorption bands of H_2CIA in the range of 1690~1247 cm^{-1} were attributed to the asymmetric and symmetric vibrations of the carboxylate groups, respectively. For Ni-CIA, the two corresponding peaks at 1690 and 1247 cm^{-1} slightly shifted to lower frequencies (1570 and 1390 cm^{-1}, respectively), which indicates that the carboxylate groups in Ni-CIA have been coordinated to the Ni^{2+} cation [54]. The crystal structure of Ni-CIA was determined via XRD analysis (Figure 1b). The XRD spectrum of Ni-CIA showed various sharp peaks, indicating the polycrystalline nature. Moreover, the main diffraction peaks of the Ni-CIA are observed at 2θ = 15.2°, 26.6°, 30.8°, 34.9°, and 40.8°, corresponding to the crystal faces of (100), (001), (110), (200), and (111), respectively.

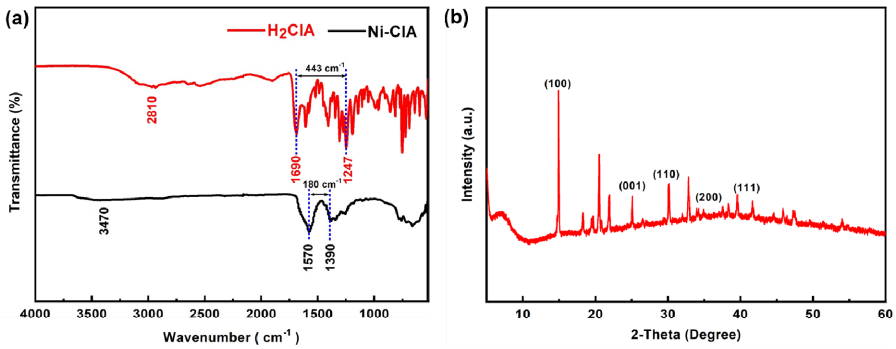

Figure 1. (**a**) FT−IR spectra of H_2CIA and Ni-CIA; (**b**) XRD pattern of Ni-CIA.

To determine the morphology of Ni-CIA, scanning electron microscopy (SEM) was carried out (Figure 2). The result indicated that Ni-CIA has a slice layer stacked combination structure, which could create a favorable environment for rapid ion diffusion and accelerate catalytic mass transfer during the catalytic process.

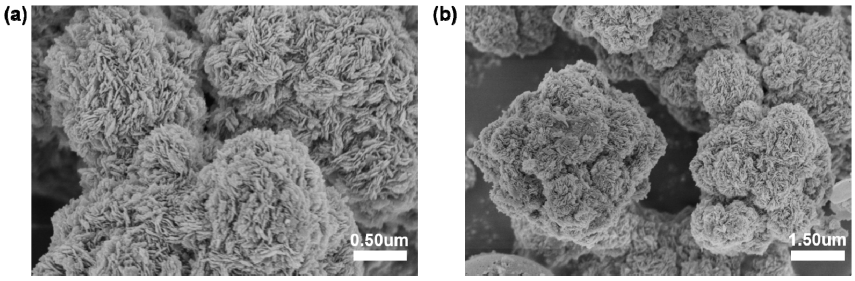

Figure 2. SEM image of (**a**,**b**) Ni-CICA.

Furthermore, XPS analysis has been performed to obtain detailed insights into the surface electronic valence states of Ni-CIA. As revealed in Figure 3a, the C 1s spectrum can be deconvoluted into five peaks [55], which were associated with C−C/C=C (284.8 eV), C−N (286.1 eV), C−O (287.0 eV), C=O (288.4 eV), and O–C=O (290.8 eV). In the N 1s spectrum of Ni-CIA (Figure 3b), three peaks with binding energies at 398.6 eV, 399.5 eV, and 400.1 eV are assigned to pyridinic-N, coordinated-N, and pyrrolic-N, respectively [56]. In Figure 3c, the high-resolution spectrum of O 1s is demonstrated. The peak is fitted into three parts at ~531.1 eV, ~532.5 eV, and ~533.3 eV, which can be accredited to Ni–O, O–H, and O–C=O, respectively [57]. Two peaks for Ni 2p (Figure 3d) are detected at binding energies 873.1 and 855.1 eV, corresponding to the Ni $2p_{1/2}$ and Ni $2p_{3/2}$, respectively. It appears that these values are consistent with the XPS data on Ni^{2+} [58]. Generally, the binding energy of coordinated-N and Ni–O were indicative of the nitrogen in H_2CIA, and oxygen in C–OH participated in the coordination during the Ni-CIA formation.

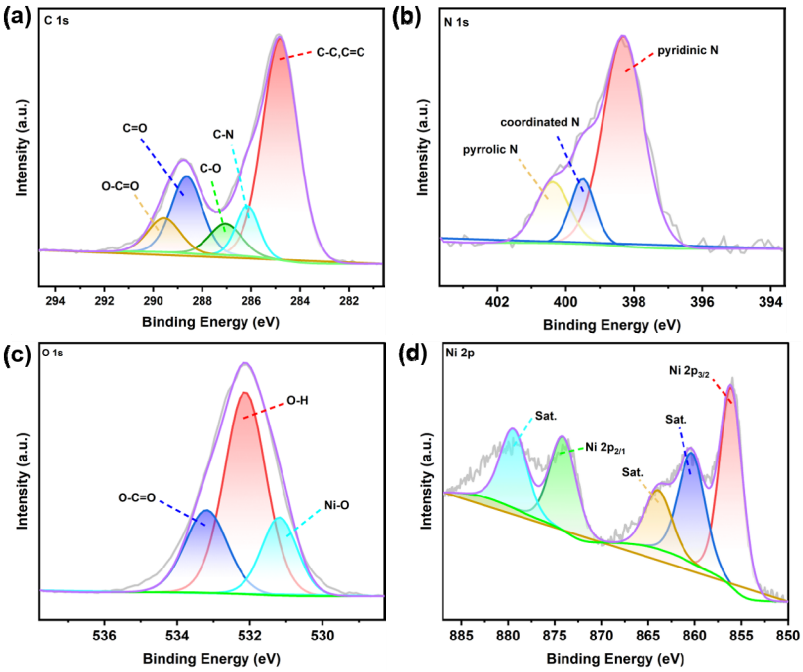

Figure 3. (**a**) High-resolution C 1s spectrum, (**b**) high-resolution N 1s spectrum, (**c**) high-resolution O 1s spectrum, and (**d**) high-resolution Ni 2p spectrum.

Further, the elemental compositional distribution determined from EDS analysis confirms the presence of C, N, O, and Ni (Figure 4a). TGA characterization was conducted and analyzed, and the corresponding results are presented in Figure 4b. For pristine Ni-CIA, 11.29% of the weight loss at ~250 °C was associated with the removal of water and decomposition of non-coordinated H_2CIA ligands. Subsequently, the coordination polymer Ni-CIA began to disintegrate, losing 49.8% of mass. The weight of Ni-CIA remains basically

stable after 400 °C. Generally, the coordination polymer Ni-CIA will not cause thermal decomposition when catalyzing reactions below 200 °C.

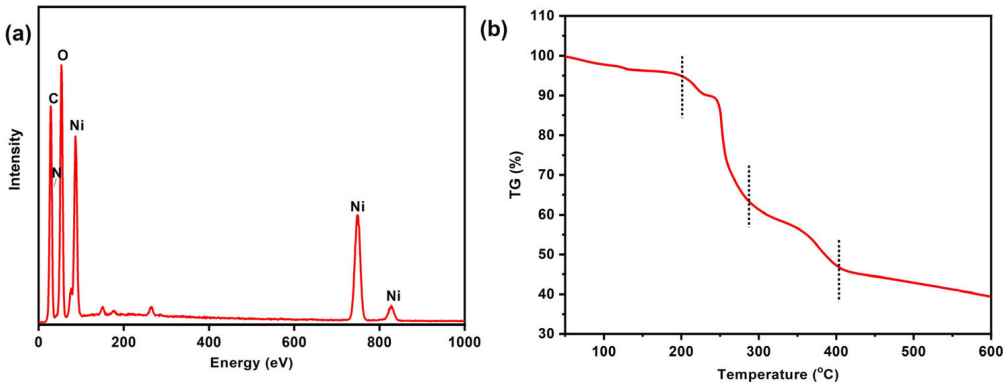

Figure 4. (**a**) EDS pattern of Ni-CIA. (**b**) TGA pattern of Ni-CIA.

2.2. Catalytic Activity

Initially, the alkylation of 2-oxindole **1a** with benzyl alcohol **2a** was chosen as a model reaction. Meanwhile, the reaction conditions were optimized as outlined in Table 1. We found that no alkylation of the desired product **3a** was observed in the absence of catalyst Ni-CIA, indicating that the Ni-CIA catalyst played a key role in this transformation (Table 1, entry 1). Various inorganic bases, including K_2CO_3, Cs_2CO_3, KO*t*Bu, KOH, and K_3PO_4, were evaluated (Table 1, entries 3–7, respectively). Among the various inorganic bases used, the best results were obtained with KO*t*Bu, which could afford the alkylation product in 84% isolated yield.

Table 1. Optimization of reaction conditions for the alkylation of 2-oxindole [a].

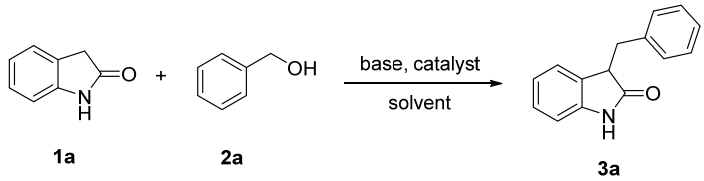

Entry	Catalyst	Base	Time [h]	Solvent	Yield [%] [b]
1	-	KO*t*Bu	6	toluene	<5
2	Ni-CIA	NEt_3	6	toluene	17
3	Ni-CIA	K_2CO_3	6	toluene	34
4	Ni-CIA	Cs_2CO_3	6	toluene	65
5	Ni-CIA	KO*t*Bu	6	toluene	84
6	Ni-CIA	KOH	6	toluene	72
7	Ni-CIA	K_3PO_4	6	toluene	56
8	Ni-CIA	KO*t*Bu	6	H_2O	<5
9	Ni-CIA	KO*t*Bu	6	1,4-dioxane	76
10	Ni-CIA	KO*t*Bu	6	xylene	80
11	Ni-CIA	KO*t*Bu	8	DMF	12
12	Ni-CIA	KO*t*Bu	2	toluene	63
13	Ni-CIA	KO*t*Bu	6	toluene	82
14 [c]	**Ni-CIA**	**KO*t*Bu**	**6**	**toluene**	**88**
15 [d]	Ni-CIA	KO*t*Bu	6	toluene	43

[a] Reaction conditions: **1a** (0.5 mmol), **2a** (1.0 mmol), catalyst (1.0 mol%), base (2.0 equiv.), and solvent (2 mL), 120 °C. [b] Isolated yields. [c] N_2. [d] O_2.

Next, we checked the reactivity of the reaction, as polar solvents such as H_2O and *N*,*N*-dimethylformamide (DMF) all led to poor yields. We then moved to non-polar solvents like xylene and 1,4-dioxane, and a slight decrease in alkylation product **3a** yield was observed

(Table 1, entries 8–11, respectively). Additionally, we attempted to adjust the reaction time; however, the yield of the desired product decreased (Table 1, entries 12–13, respectively). Subsequently, the reaction was carried out under a N_2 atmosphere, affording the target product **3a** in excellent yield (88% yield) (Table 1, entry 14). Finally, the O_2 atmosphere was screened, though with a greatly reduced yield of 43% (Table 1, entry 15).

With the optimized reaction conditions in hand, the substrate scope of benzyl alcohol was then investigated. We were pleasantly surprised to find that 2-oxindole **1a** reacted with benzyl alcohol derivatives **2** smoothly to afford the desired product **3** in moderate to excellent yields. However, the electronic effect of the substituents on the benzene ring had slight distinctions. When a variety of electron-withdrawing groups (such as -F, -Cl, -Br, and -CF_3) were present at the *para*-position, the corresponding products were obtained in good to excellent yields (Scheme 2, entries **3d**–**3g**). In contrast, when a variety of electron-donating groups (such as -Me, -OMe, and -*t*Bu) were attached to the *para*-position (Scheme 2, entries **3b**, **3c**, and **3h**), the desired product was obtained in moderate yields. In comparison, slightly lower yields were observed at the *meta*-, *ortho*-position of the benzene ring of benzyl alcohols substituents (**3i**–**3l**), which are probably due to steric hindrance. To our delight, even if the electronic effect was enhanced through adding substituents (-CF_3) on the benzene ring, the yield of the desired product was not reduced (**3m**). Subsequently, several heteroaryl primary alcohols, including 2-naphthalenemethanol, 2-thiophenemethanol, and piperonyl alcohol, were also investigated (**3n**–**3p**). To our delight, they were still compatible, and the desired products were obtained in good yields. The scope was further extended to linear aliphatic secondary alcohols. Interestingly, aliphatic alcohols were also effective for the alkylation of 2-oxindole to offer the corresponding products **3q**–**3s** in moderate yields. Meanwhile, alicyclic alcohol (cyclopropane methanol **2t**) was also effective at yielding the corresponding products 3-(cyclopropyl methyl)indolin-2-one **3t** in good yields.

Furthermore, we were eager to explore more synthetic utilities that the Ni-CIA catalyst has to offer, since the quinoline framework is a crucial class of heterocyclic scaffolds, which could be found in many natural products, drugs, and advanced functional materials [59–61]. Therefore, exploring new methods for synthesizing quinoline derivatives has become a research hotspot in the field of organic synthesis [62–68]. To our delight, using Ni-CIA as a catalyst, we have achieved an effective method to synthesize quinoline derivatives via borrowing hydrogen transformation. Meanwhile, we further explored the substrate scope of this process (Scheme 3). A series of acetophenones bearing different groups were investigated. Almost all the acetophenones reacted with *o*-aminobenzyl alcohol smoothly to produce quinoline derivatives with good to excellent yields. We can find that when using acetophenone **5** with electron-donating substituents, higher yields could be achieved than their counterparts with electron-withdrawing substituents (Scheme 3, entries **6a**–**6f**). During the transformation, compared to the *para*-position of the benzene ring of acetophenone substituents, a slight decrease in the yield of acetophenone substituents in the *meta*- and *ortho*- positions of the benzene ring was noticed during this transformation (Scheme 3, entries **6g**–**6j**). Heteroaromatic alcohols with a pyridinyl group also afforded the corresponding indoles in 72% yield (Scheme 3, entry **6m**). Interestingly, we observed that alkyl ketones could be well tolerated in the reaction of *o*-aminobenzyl alcohol with ketone, affording moderate yields (Scheme 3, entries **6n**, **6o**).

2.3. Mechanism Explorations

To gain insight into the mechanism of the alkylation of 2-oxindole with alcohols, several catalyst investigative experiments were conducted (Table 2). Firstly, four different commercially available simple nickel salts were examined. The control experiments were carried out with KO*t*Bu as a base, dissolved in toluene for 6 h (Table 2, entries 1–4). It was found that almost no reaction occurred when simple nickel salts were employed. Meanwhile, a low yield was observed when Ni-complexes were used as catalysts (Table 2, entries 5–6). These results reveal that the Ni-CIA catalyst has played a crucial role in the transformation.

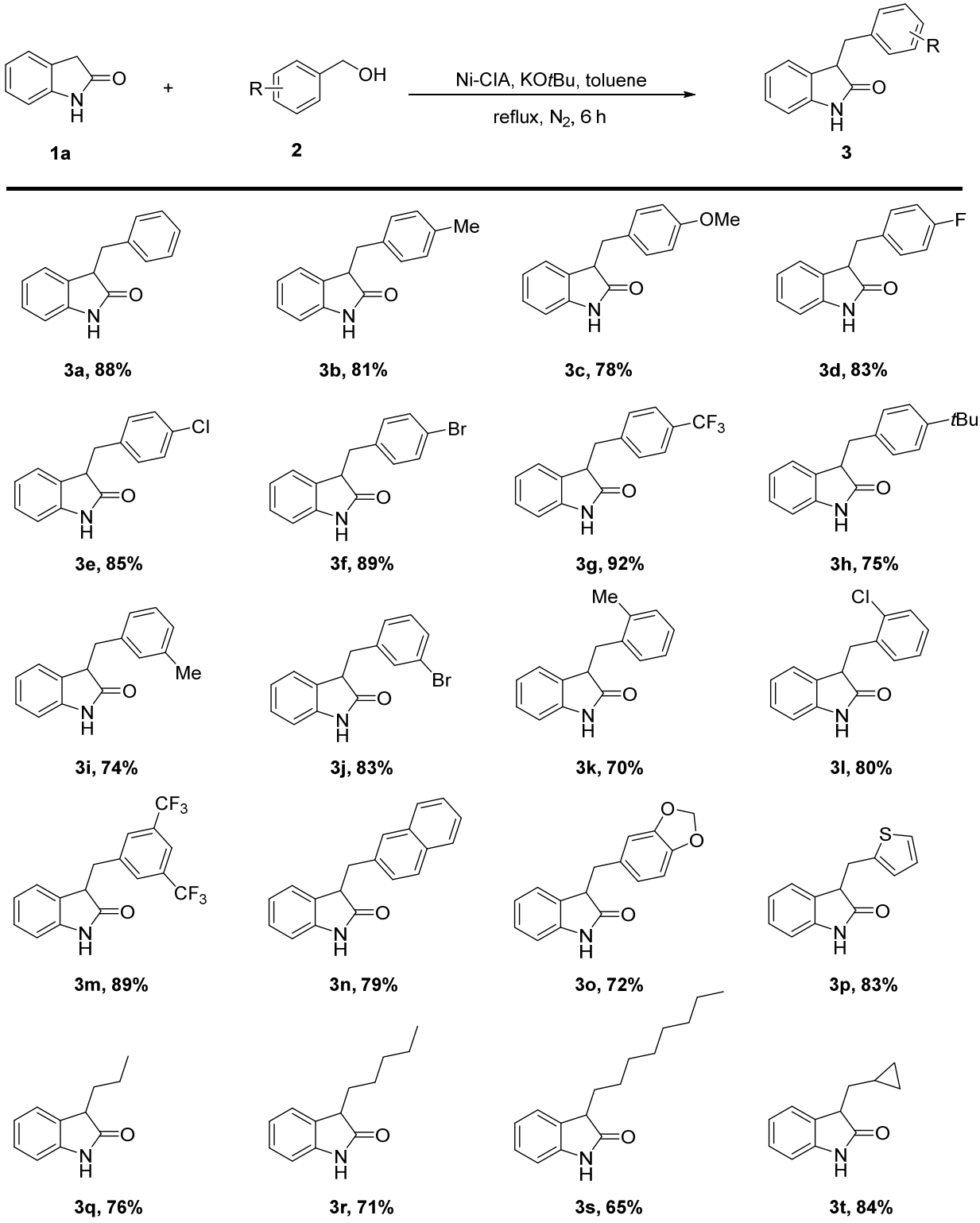

Scheme 2. Alkylation of 2-oxindole with alcohols [a,b]. [a] Reaction conditions: **1a** (0.5 mmol), **2a** (1.0 mmol), Ni-CIA (1.0 mol%), KO*t*Bu (2.0 equiv.), and toluene (2 mL), N_2,6 h, 120 °C. [b] Isolated yields.

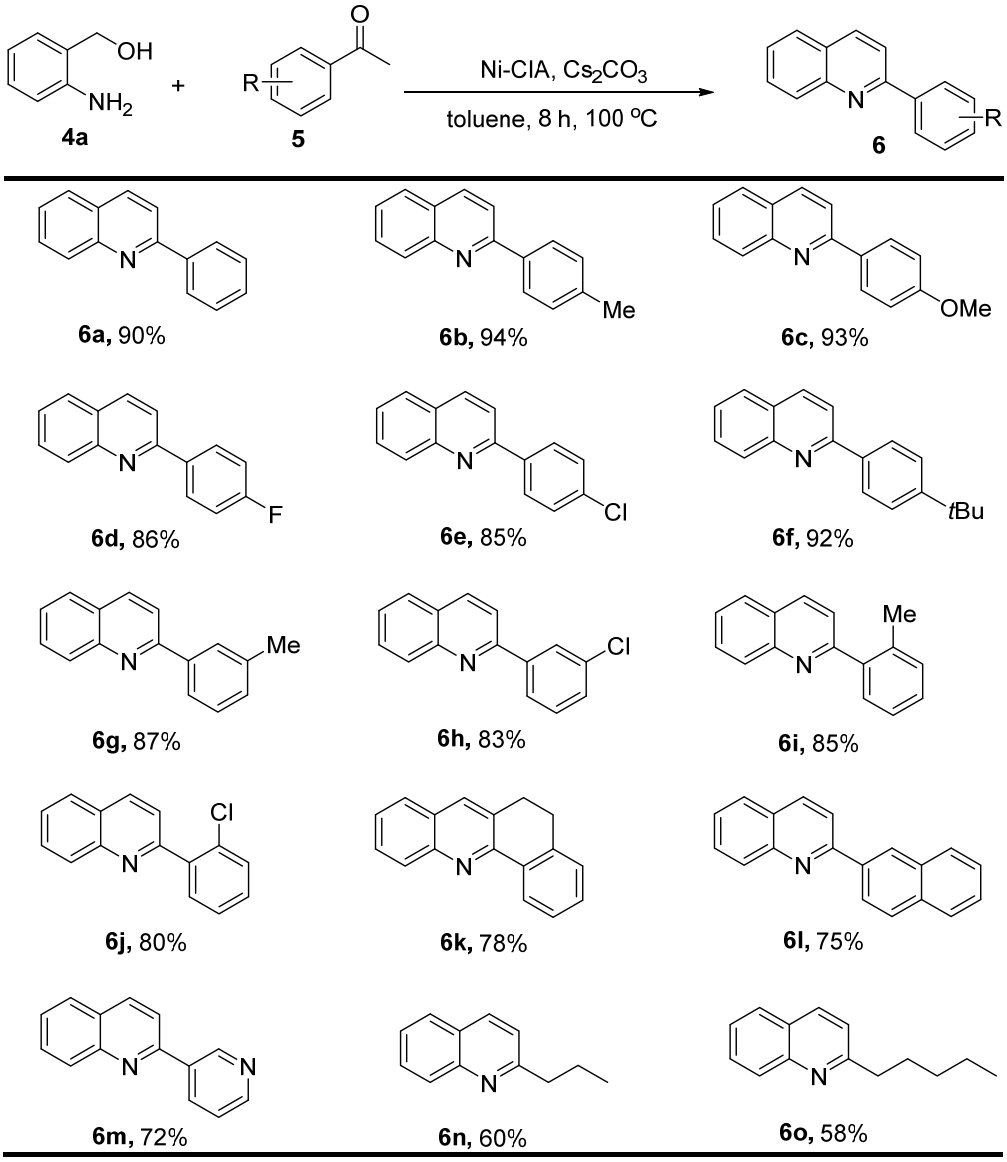

Scheme 3. Ni-CIA-catalyzed reaction of acetophenones with *o*-aminobenzyl alcohol [a,b]. [a] Reaction conditions: **4a** (0.5 mmol), **5** (0.6 mmol), Ni-CIA (1.0 mol%), Cs_2CO_3 (1.0 equiv.), and toluene (2 mL), 100 °C, 8 h. [b] Isolated yields.

Table 2. Catalyst investigation experiments [a,b].

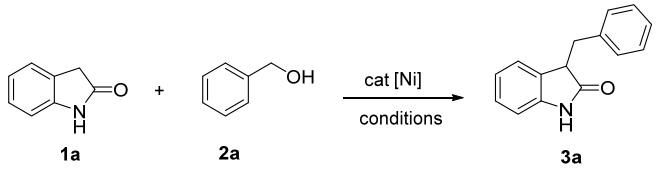

Entry	Catalyst	Yield [%] [b]	Entry	Catalyst	Yield [%] [b]
1	$NiCl_2 \cdot 6H_2O$	15	5	$NiCl_2(bipy)_2$	32
2	$NiBr_2 \cdot 3H_2O$	<5	6	$NiCl_2(phen)_2$	45
3	$Ni(NO_3)_2 \cdot 6H_2O$	<5	7	Ni-CIA	88
4	$Ni(OAc)_2 \cdot 6H_2O$	<5	8	none	<5

[a] Reaction conditions: **1a** (0.5 mmol), **2a** (1.0 mmol), catalyst (1.0 mol%), KO*t*Bu (2.0 equiv.), and toluene (2 mL), N_2, 6 h, 120 °C. [b] Isolated yields.

In order to better understand the mechanism of this transformation and to clarify the effect of different substituents on reactivity, several control experiments were subsequently carried out. When benzyl alcohol containing electron-donating or electron-withdrawing groups (**2c** vs. **2g**) reacted with 2-oxindole (**1a**) for 2 h under optimal conditions, the experiment results indicated that the molar ratio of two products (**3c** vs. **3g**) was found to be 1:2.4, indicating that the electron-deficient alcohol was preferentially consumed. Meanwhile, it is concluded that benzyl alcohol with an electron-withdrawing group was much more reactive than that with an electron-donating group for this reaction (Scheme 4).

Further mechanism exploration was also executed using two useful types of radical scavenger, 2,2,6,6-tetramethyl-1-piperidinyloxy (TEMPO, 1.0 equiv.) and 2,6-ditert-butyl-4-methylphenol (BHT, 1.0 equiv.), to test and verify the possibility of the radical process in this reaction (Scheme 5a). The experimental results showed that the reaction of 2-oxindole 1a and benzyl alcohol **2a** produced the desired products **3a** in 76% and 84% yields, respectively, and ruled out the possibility of a radical pathway during this Ni-CIA-catalyzed reaction.

In order to find out the right reaction pathway, we next carried out several control experiments to capture possible intermediates (Scheme 5b). When only benzyl alcohol **2a** was used as the reactant, the intermediate benzaldehyde **2a′** was formed with a yield of 64% under optimal conditions, which indicated that the Ni-CIA catalyst was essential for the oxidation of benzyl alcohol **2a** (i). Furthermore, the reaction of benzaldehyde **2a′** and 2-oxindole **1a** afforded an α,β-unsaturated amide **1a′** with 92% yield (ii). At the same time, the experimental results indicate that α,β-unsaturated amide **1a′** and benzyl alcohol **2a** could not react to form desired product **3a** without the participation of the Ni-CIA catalyst, implying that the Ni-CIA catalyst was necessary for this transformation (iii).

Subsequently, to understand the mechanism of **6a** formation, a series of control experiments were performed (Scheme 6). Initially, in the presence of BTH and TEMPO, this transformation proceeded well, and the yield of **6a** was only slightly decreased. This rules out the involvement of an organic radical intermediate during this reaction, as it is widely accepted that the capture of key intermediate is an efficient and reliable way to explain what happened in this reaction process. The reaction of only *o*-aminobenzyl alcohol **4a** produced 2-aminobenzaldehyde **4a′** in 58% isolated yield under the standard conditions (i). The reaction of 2-aminobenzaldehyde **4a′** and acetophenone **5a** afforded the 2-phenylquinoline **6a** in 94% yield in the absence of catalyst Ni-CIA, implying that the carbonyl compound (2-aminobenzaldehyde **4a′**) is the intermediate, and Cs_2CO_3 played a significant role in the deprotonation of alcohols and condensation (ii). Notably, the formation of 2-phenylquinoline **6a** was not observed from the coupling of *o*-aminobenzyl alcohol **4a** with acetophenone **5a** in the absence of the catalyst (iii). The above control experiment results together confirmed that the catalyst Ni-CIA facilitated the dehydrogenation of the *o*-aminobenzyl alcohol **4a** and that 2-aminobenzaldehyde **4a′** was the intermediate in this process.

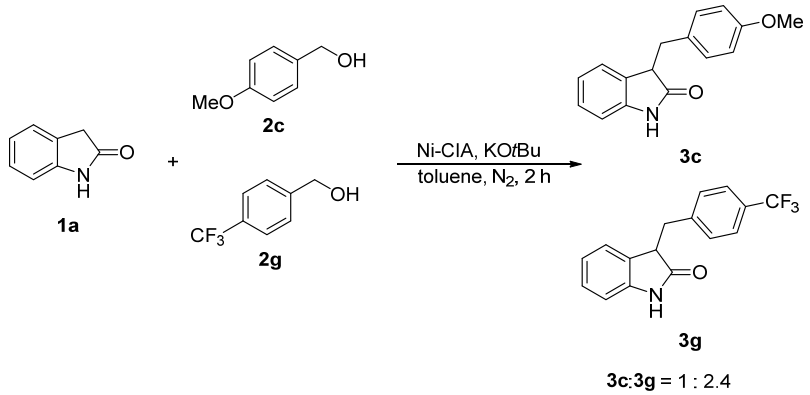

Scheme 4. The control experiments.

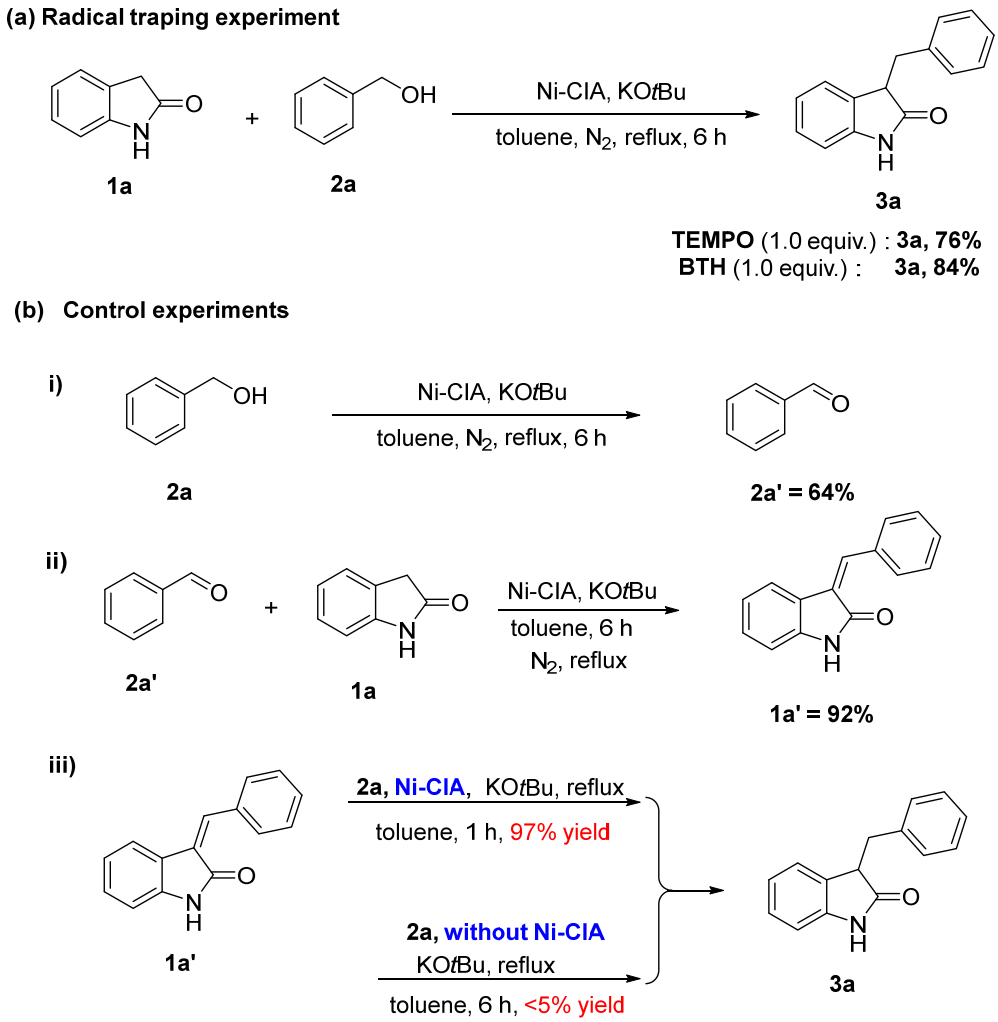

Scheme 5. Mechanism exploration experiments.

Based on our experimental research and previous literature, a possible mechanism is proposed in Scheme 7 [33–37]. First, the catalyst Ni-CIA undergoes an ion exchange with the base KO*t*Bu to produce the active species **A**, which then participates in the catalytic cycle. Subsequently, **A** reacts with benzyl alcohol **2a**, which results in the formation of alkoxy intermediate **B**. The intermediate complex **B** undergoes β-hydride elimination of alkoxide to generate the dehydrogenated product benzaldehyde **2a′** with the formation of [Ni-H] species. After that, the benzaldehyde **2a′** reacted with 2-oxindole **1a** to form an α,β-unsaturated amide **1a′** intermediate. Finally, α,β-unsaturated amide **1a′** was reduced by the [Ni-H] species. Meanwhile, **A** was regenerated to complete the catalytic cycle.

Similarly, a plausible mechanism for the Ni-catalyzed synthesis of quinoline derivatives via the dehydrogenative coupling of *o*-aminobenzyl alcohol **4a** with acetophenone **5a** is shown in Scheme 8. Firstly, the deprotonation of **4a** assisted by the Cs_2CO_3 produces the active species **C**, which then participate in this catalytic cycle. Next, **C** reacted with Ni-CIA to afford the alkoxy intermediate **D**. The intermediate **D** undergoes β-hydride elimination of alkoxide to produce the dehydrogenated product 2-aminobenzaldehyde **4a′** with the formation of [Ni-H] species. Subsequently, 2-aminobenzaldehyde **4a′** undergoes base-catalyzed cross-aldol condensation reaction with acetophenone **5a** to form an α,β-unsaturated ketone. Finally, the α,β-unsaturated ketone reacts via intramolecular cyclization to produce the product **6a**.

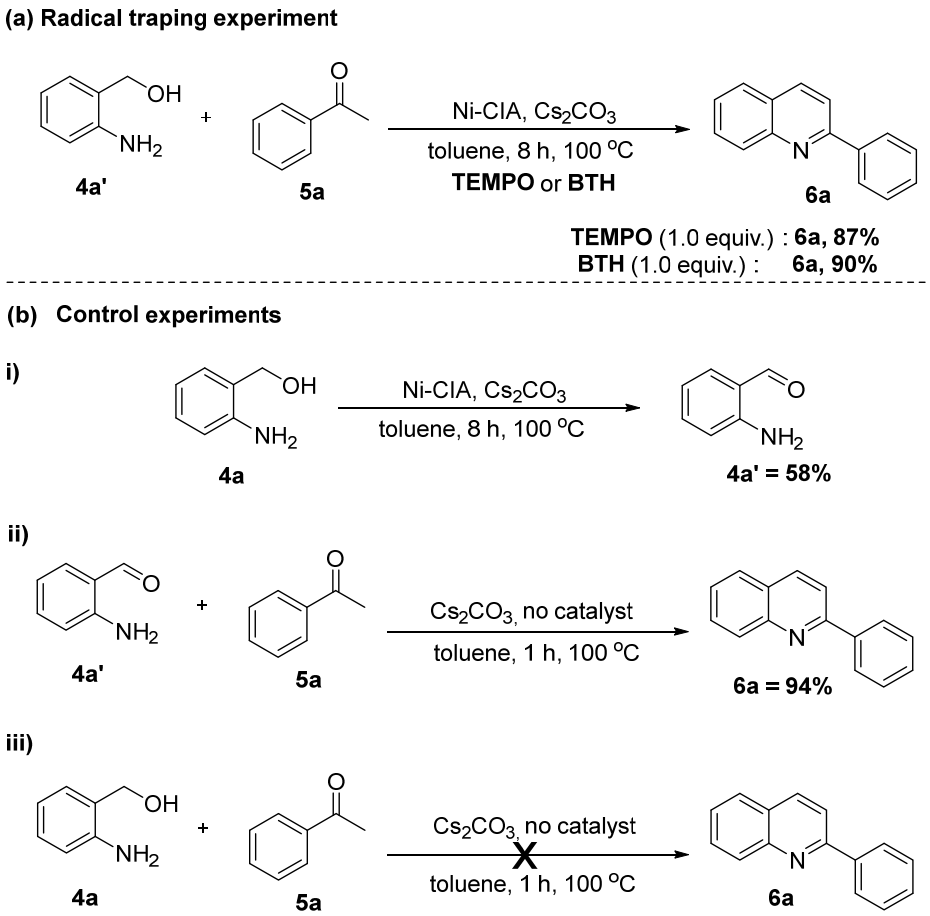

Scheme 6. Mechanism exploration experiments for the synthesis of quinolines.

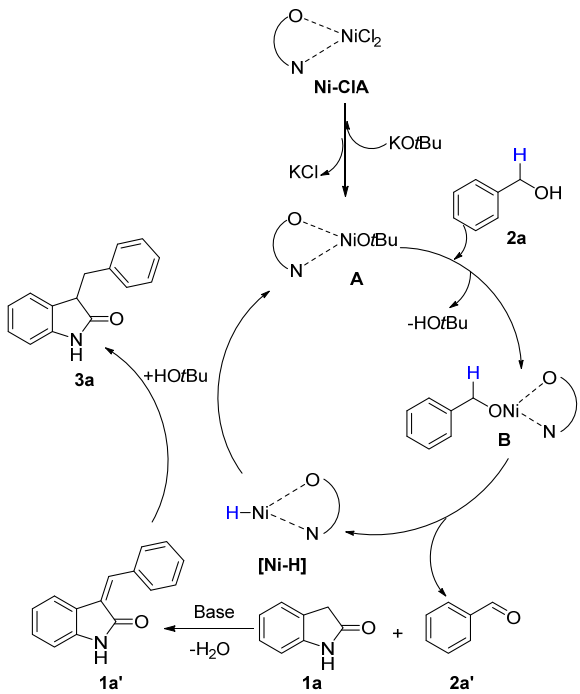

Scheme 7. Proposed possible reaction mechanism.

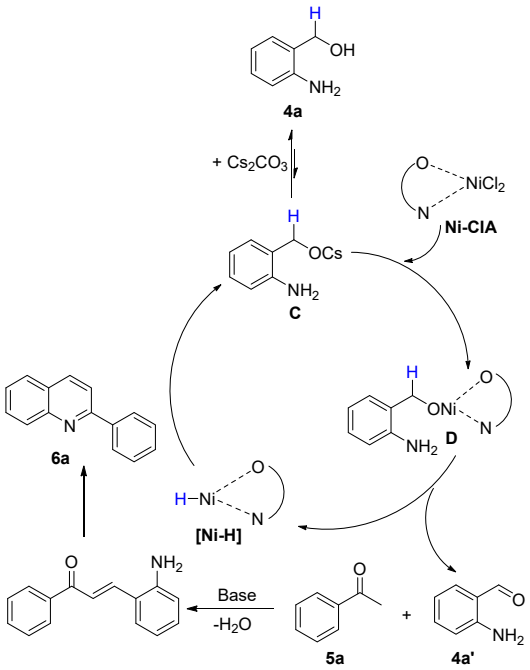

Scheme 8. Proposed possible reaction mechanism for the synthesis of quinolines.

2.4. Reusability of the Catalyst

Finally, the durability of the catalyst Ni-CIA was assessed through recycling experiments. After the reaction of 2-oxindole **1a** with benzyl alcohol **2a**, the heterogeneous catalyst Ni-CIA was conveniently separated from the reaction mixture via centrifugation, followed by washing with methanol, deionized water, and ethanol, respectively, and dried at 80 °C for 12 h. Then, it was reused in the following run without any pre-treatment, as shown in Scheme 9. To our delight, the catalyst Ni-CIA provided a high yield of **3a** even after the fifth recycling experiment. Meanwhile, after the reaction cycle, the leaching of Ni species was measured via ICP-MS analysis. It was shown that the leaching of Ni species in this reaction solution was only 5.2 μg/L, which disclosed that the heterogeneous catalyst Ni-CIA had good stability. After the recycling experiments, the Ni-CIA catalyst was collected and characterized via scanning electron microscopy (SEM) again after being washed three times with methanol, deionized water, and ethanol and dried at 80 °C (Figure S1). From the figure, no significant change in the morphology of the catalyst Ni-CIA is seen, retaining its slice layer stacked combination structure.

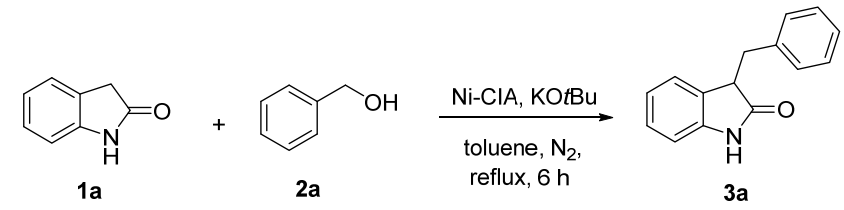

Recycled times	0	1	2	3	4
Yields	88%	83%	80%	80%	77%

Scheme 9. Recycling experiments.

3. Materials and Methods

3.1. Catalyst Characterization

All reactions that require air and/or moisture-sensitive conditions were carried out under a nitrogen atmosphere using oven/flame-dried glassware and standard syringe/septa

techniques. Unless otherwise noted, all commercial reagents and solvents were obtained from the commercial provider and used without further purification. FT-IR spectra (Thermo Fisher Co., Waltham, MA, USA) were recorded on a Nicolet 360 FT-IR instrument (KBr discs) in the 4000–525 cm^{-1} regions. SEM and EDS (Hitachi, Tokyo, Japan) was performed on a HITACHI S-4800 field-emission scanning electron microscope. TG analysis was carried out using an STA409 (Mettler-Toli, Greifensee, Switzerland) instrument in N_2 at a heating rate of 10 °C/min from 50 to 800 °C. XRD patterns were collected on a Bruker D8 (Bremen, Germany) Advance powder diffractometer, using a Ni-filtered Cu/Kα radiation source at 40 kV and 20 mA, from 5° to 90° with a scan rate of 4°/min. XPS data were recorded with an electron energy analyzer (ESCALAB 250Xi, Thermo Fisher Co., Waltham, MA, USA). Flash column chromatography was performed on 230–430 mesh silica gel. Analytical thin layer chromatography was performed with precoated glass baked plates (250 μ) and visualized via fluorescence and charring after treatment with potassium permanganate stain. ^{1}H NMR and ^{13}C NMR spectra were obtained on a Bruker Advance III HD (Zurich, Switzerland) 400 MHz spectrometer and referenced to $CDCl_3$ (7.26 ppm for ^{1}H, and 77.1 ppm for ^{13}C) or DMSO-d_6 (2.50 ppm for ^{1}H, and 39.5 ppm for ^{13}C) with tetramethylsilane as the internal standard (0 ppm).

3.2. Chemicals

The following chemicals were used as received: methyl indole-5-carboxylate (>98%, Adamas, Shanghai, China), methyl 2-bromoacetate (>98%, Adamas), anhydrous potassium carbonate (K_2CO_3, >99%, Sinopharm, Beijing, China), anhydrous magnesium sulfate ($MgSO_4$, >99%, Sinopharm), acetonitrile (MeCN, 99.9%, Sigma, Shanghai, China), $LiOH{\cdot}H_2O$ (>95%, Sinopharm, Beijing, China), Tetrahydrofuran (THF, 99.9%, Sigma, Shanghai, China), $NiCl_2.6H_2O$ (Adamas, Shanghai, China), *N*,*N*-dimethylformamide (DMF, 99.9%, Sigma, Shanghai, China), ethanol (99%, Sigma, Shanghai, China), KO*t*Bu (>98%, Sinopharm, Beijing, China), 2-oxindole derivative (>98%, Adamas, Shanghai, China), benzyl alcohol derivatives (>99%, Adamas, Shanghai, China), *o*-aminobenzyl alcohol (99%, Sigma, Shanghai, China), acetophenone derivatives (>99%, Adamas, Shanghai, China). Unless otherwise noted, all commercial reagents and solvents were obtained from the commercial provider and used without further purification.

3.3. Catalyst Preparation

To a 500 mL round-bottom bottle, we successively added methyl indole-5-carboxylate (3.504 g, 20 mmol), methyl 2-bromoacetate (7.649 g, 50 mmol), anhydrous potassium carbonate (11.057 g, 80 mmol), and MeCN (100 mL). The reaction mixture was refluxed for 20 h and monitored via thin layer chromatography (TLC) until the complete disappearance of methyl indole-5-carboxylate was confirmed. Then, the mixture was extracted with water and ethyl acetate. The combined organic phases were washed and dried over anhydrous $MgSO_4$. The solvent was removed using a rotary evaporator under reduced pressure, and the crude product was purified via column chromatography on silica gel to afford methyl 1-(2-methoxy-2-oxoethyl)-1*H*-indole-5-carboxylate in 88% yield as a pale yellow solid. ^{1}H NMR (400 MHz, $CDCl_3$) δ 8.43 (s, 1H), 7.96 (d, *J* = 10.3 Hz, 1H), 7.28 (d, *J* = 6.8 Hz, 1H), 7.17 (d, *J* = 3.3 Hz, 1H), 6.69 (d, *J* = 4.0 Hz, 1H), 4.91 (s, 2H), 3.95 (s, 3H), 3.78 (s, 3H). ^{13}C NMR (101 MHz, $CDCl_3$) δ 168.58, 168.04, 138.98, 129.83, 128.22, 124.13, 123.56, 122.16, 108.64, 104.08, 52.65, 51.85, 47.79.

To a mixed solution of THF–water (*v*/*v* = 1:1) (200 mL) and $LiOH{\cdot}H_2O$ (40 mL), we successively added 1-(2-methoxy-2-oxoethyl)-1*H*-indole-5-carboxylate (20 mmol) in THF/water (*v*/*v* = 1:1) (200 mL) at room temperature and at 800 rpm. After stirring for 4 h, the reaction system was acidified to pH = 2 through adding an aqueous solution of 1M HCl. The product, 1-(carboxymethyl)-1*H*-indole-5-carboxylic acid (H_2CICA), was washed with water, then evaporated to dry, obtaning a pale yellow solid in 95% yield (Scheme 10). ^{1}H NMR (400 MHz, DMSO-d_6) δ 12.58 (s, 2H), 8.04 (m, 2H), 7.48 (d, *J* = 7.0 Hz, 1H), 7.22 (m,

2H), 5.13 (s, 2H). ^{13}C NMR (101 MHz, DMSO-d_6) δ 170.32, 166.05, 137.45, 136.82, 126.74, 122.81, 121.81, 121.19, 111.14, 107.46, 47.80.

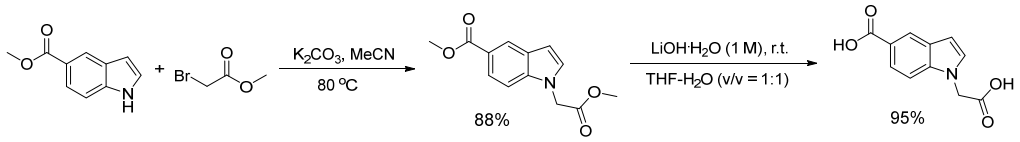

Scheme 10. The synthesis of H_2CICA.

A mixture of $NiCl_2.6H_2O$ (0.237 g, 1.0 mmol) and H_2CIA (0.219 g, 1.0 mmol) was dissolved in a 5:2:1 ($v/v/v$) DMF/ethanol/water mixture of (8 mL) in a 15 mL Teflon reactor. The mixture was heated in an oven at 110 °C for 48 h and then cooled to room temperature. The obtained mixture was filtered, successively washed with DMF/ethanol/water and ethanol twice, and finally heated at 80 °C for 5 h to produce a green powder (Ni-CIA).

3.4. Alkylation of 2-Oxindole with Alcohols

A mixture of Ni-CIA (1.0 mol%), **1** (0.5 mmol), **2** (1.0 mmol), KO*t*Bu (2.0 equiv.), and toluene (2.0 mL) was stirred in a 20 mL Schlenk tube under N_2 at 120 °C for 6 h. The reaction mixture was cooled down to room temperature, then removed via filtration to obtain the residue. The residue was then directly purified via column chromatography with petroleum ether/ethyl acetate as eluent to produce the desired product.

3.5. Reaction of Synthesis of Quinoline Derivatives

A mixture of Ni-CIA (1.0 mol%), **4** (0.5 mmol), **5** (0.6 mmol), Cs_2CO_3 (1.0 equiv.) and toluene (2.0 mL) was stirred in a 20 mL Schlenk tube under 100 °C for 8 h. The reaction mixture was cooled down to room temperature, then removed via filtration to produce the residue. The residue was then directly purified via column chromatography with petroleum ether/ethyl acetate as eluent to yield the desired product.

4. Conclusions

In summary, we herein report a simple, effective, and reusable heterogeneous coordination polymer Ni-CIA catalyst for promoting the synthesis of oxindole and quinoline derivatives through the borrowing hydrogen strategy. The slice layer stacked combination structure of the catalyst can effectively promote ion diffusion and accelerate catalytic mass transfer during the catalytic reaction. Moreover, various primary alcohol and acetophenone substrates were tested under optimized reaction conditions to form the desired compounds in moderate to excellent yields. After that, mechanism explorations including control experiments were conducted to clarify the effect of different substituents, and cooperative effects were investigated to clarify these transformations. The above experimental results confirmed that catalysis with Ni-CIA facilitates the dehydrogenation of the benzyl alcohol **2a** and *o*-aminobenzyl alcohol **4a**, revealing that the reaction followed the hydrogen-borrowing mechanism; thus, we proposed possible reaction mechanisms for the two types of reactions. Finally, the recycling experiments showed that the Ni-CIA catalyst had fine stability. In particular, it was shown that no significant reduction in activity and no significant changes in surface morphology were observed for Ni-CIA after five runs. This catalytic system is shown as a much greener method for the synthesis of oxindole and quinoline derivatives, in accordance with the principles of sustainable development and atom economy, making it highly promising for organic catalysis.

Supplementary Materials: The following supporting information can be downloaded at: https://www.mdpi.com/article/10.3390/catal13081195/s1, Figure S1: (a) and (b) SEM image of Ni-CIA after being recycled five times, Analytical data of the obtained compounds. References [69,70] are cited in the Supplementary Materials.

Author Contributions: Conceptualization, J.L.; methodology, J.L. and J.T.; validation, J.L., J.T. and L.W.; formal analysis, J.L. and J.T.; investigation, J.T. and L.W.; resources, D.W. and Z.-C.D.; writing—original draft preparation, J.L.; writing—review and editing, D.W.; visualization, D.W. and Z.-C.D.; supervision, D.W. and Z.-C.D.; project administration, D.W.; funding acquisition, D.W. All authors have read and agreed to the published version of the manuscript.

Funding: This research was funded by the National Natural Science Foundation of China (No. 21861039).

Acknowledgments: We gratefully acknowledge financial support of this work by the National Natural Science Foundation of China (21861039) and Central Laboratory, School of Chemical and Material Engineering, Jiangnan University.

Conflicts of Interest: The authors declare no conflict of interest.

References

1. Jiang, T.; Kuhen, K.L.; Wolff, K.; Yin, H.; Bieza, K.; Caldwell, J.; Bursulaya, B.; Wu, T.Y.; He, Y. Design, synthesis and biological evaluations of novel oxindoles as HIV-1 non-nucleoside reverse transcriptase inhibitors. Part I. *Bioorg. Med. Chem. Lett.* **2006**, *16*, 2105–2108. [CrossRef] [PubMed]
2. Wang, H.; Chen, M.; Wang, L. Selective Synthesis and Utility of One Tripyrrolic Compound and Its Intermediates. *Chem. Pharm. Bull.* **2007**, *55*, 1439–1441. [CrossRef]
3. Reisman, S.E.; Ready, J.M.; Weiss, M.M.; Hasuoka, A.; Hirata, M.; Tamaki, K.; Ovaska, T.V.; Smith, C.J.; Wood, J.L. Evolution of a Synthetic Strategy: Total Synthesis of (±)-Welwitindolinone A Isonitrile. *J. Am. Chem. Soc.* **2008**, *130*, 2087–2100. [CrossRef] [PubMed]
4. Rodrigues, T.; Reker, D.; Schneider, P.; Schneider, G. Counting on natural products for drug design. *Nat. Chem.* **2016**, *8*, 531–541. [CrossRef]
5. Huang, L.; Yang, L.; Wan, J.P.; Zhou, L.; Liu, Y.; Hao, G. Metal-free three-component assemblies of anilines, alpha-keto acids and alkyl lactates for quinoline synthesis and their anti-inflammatory activity. *Org. Biomol. Chem.* **2022**, *20*, 4385–4390. [CrossRef] [PubMed]
6. Liu, H.; Zeng, X.-Q.; Zuo, H.-W.; Zhang, N.; Huang, Z.-Y. Design, Synthesis and Seed Germination Inhibition Activity of Quinoline-6-sulfonamide Compounds. *Chin. J. Org. Chem.* **2022**, *42*, 2947–2953. [CrossRef]
7. Moutaouakil, M.; Tighadouini, S.; Almarhoon, Z.M.; Al-Zaben, M.I.; Bacha, A.B.; Masand, V.H.; Jamaleddine, J.; Saddik, R. Quinoline Derivatives with Different Functional Groups: Evaluation of Their Catecholase Activity. *Catalysts* **2022**, *12*, 1468. [CrossRef]
8. Hu, C.; Lu, L.; Wan, J.P.; Wen, C. The Pharmacological Mechanisms and Therapeutic Activities of Hydroxychloroquine in Rheumatic and Related Diseases. *Curr. Med. Chem.* **2017**, *24*, 2241–2249. [CrossRef]
9. Trost, B.M.; Zhang, Y. Molybdenum-Catalyzed Asymmetric Allylation of 3-Alkyloxindoles: Application to the Formal Total Synthesis of (−)-Physostigmine. *J. Am. Chem. Soc.* **2006**, *128*, 4590–4591. [CrossRef]
10. Kende, A.S.; Hodges, J.C. Regioselective C-3 Alkylations of Oxindole Dianion. *Synth. Commun.* **2007**, *12*, 1–10. [CrossRef]
11. Chaudhari, M.B.; Sutar, Y.; Malpathak, S.; Hazra, A.; Gnanaprakasam, B. Transition-Metal-Free C-H Hydroxylation of Carbonyl Compounds. *Org. Lett.* **2017**, *19*, 3628–3631. [CrossRef] [PubMed]
12. Chakraborty, S.; Daw, P.; David, Y.B.; Milstein, D. Manganese-Catalyzed alpha-Alkylation of Ketones, Esters, and Amides Using Alcohols. *ACS Catal.* **2018**, *8*, 10300–10305. [CrossRef]
13. Duan, Y.T.; Wang, Z.X. Transition-Metal-Free α-C-Alkylation of Oxindoles with Alcohols. *Asian J. Org. Chem.* **2023**, *12*, e202300015. [CrossRef]
14. Luo, X.; Tian, A.; Pei, M.; Yan, J.; Liu, X.; Wang, L. Highly Stable Univalent Copper of a Cu@Al/SBA-15 Nanocomposite Catalyzes the Synthesis of Fluorescent Aminobenzotriazoles Derivatives. *Chem. Eur. J.* **2022**, *28*, e202103361. [CrossRef] [PubMed]
15. Wang, D.; Xia, X.; Hu, W.; Yang, Y.; Li, J. Catalytic Synthesis of Pyrazine and Ketone Derivatives by Unsymmetrical Triazolyl-Naphthyridinyl-Pyridine Copper. *Chin. J. Org. Chem.* **2022**, *42*, 190–199. [CrossRef]
16. Pena-Lopez, M.; Piehl, P.; Elangovan, S.; Neumann, H.; Beller, M. Manganese-Catalyzed Hydrogen-Autotransfer C-C Bond Formation: Alpha-Alkylation of Ketones with Primary Alcohols. *Angew. Chem. Int. Ed. Engl.* **2016**, *55*, 14967–14971. [CrossRef]
17. Li, J.; Mao, A.; Yao, W.; Zhu, H.; Wang, D. Iridium supported on porous polypyridine-oxadiazole as high-activity and recyclable catalyst for the borrowing hydrogen reaction. *Green Chem.* **2022**, *24*, 2602–2612. [CrossRef]
18. Wang, D.; Ge, B.; Zhang, B.; Liu, H.; Li, J. Synthesis of Supported Indazolyl-Pyridyl-Quinoline Iridium Catalyst and Its Application to *N*-Alkylation of 2-Aminobenzothiazoles. *Chin. J. Org. Chem.* **2022**, *42*, 619–630. [CrossRef]
19. Banik, A.; Datta, P.; Mandal, S.K. C-Alkylation by Phenalenyl-Based Molecule via a Borrowing Hydrogen Pathway. *Org. Lett.* **2023**, *25*, 1305–1309. [CrossRef]
20. Chen, X.; Liu, D.; Yang, C.; Shi, L.; Li, F. Hexaazatrinaphthalene-Based Covalent Triazine Framework-Supported Rhodium(III) Complex: A Recyclable Heterogeneous Catalyst for the Reductive Amination of Ketones to Primary Amines. *Inorg. Chem.* **2023**, *62*, 9360–9368. [CrossRef]

21. Liu, Y.; Diao, H.; Hong, G.; Edward, J.; Zhang, T.; Yang, G.; Yang, B.M.; Zhao, Y. Iridium-Catalyzed Enantioconvergent Borrowing Hydrogen Annulation of Racemic 1,4-Diols with Amines. *J. Am. Chem. Soc.* **2023**, *145*, 5007–5016. [CrossRef]
22. Ng, T.W.; Tao, R.; See, W.W.L.; Poh, S.B.; Zhao, Y. Economical Access to Diverse Enantiopure Tetrahydropyridines and Piperidines Enabled by Catalytic Borrowing Hydrogen. *Angew. Chem. Int. Ed.* **2023**, *62*, e202212528. [CrossRef] [PubMed]
23. Hamid, M.H.S.A.; Slatford, P.A.; Williams, J.M.J. Borrowing Hydrogen in the Activation of Alcohols. *Adv. Synth. Catal.* **2007**, *349*, 1555–1575. [CrossRef]
24. Nakayama, T.; Harada, S.; Kikkawa, S.; Hikawa, H.; Azumaya, I. Palladium-Catalyzed Dehydrogenative Synthesis of Imidazoquinolines in Water. *Asian J. Org. Chem.* **2022**, *11*, e202200510. [CrossRef]
25. Putra, A.E.; Takigawa, K.; Tanaka, H.; Ito, Y.; Oe, Y.; Ohta, T. Transition-Metal-Catalyzed Regioselective Alkylation of Indoles with Alcohols. *Eur. J. Org. Chem.* **2013**, *2013*, 6344–6354. [CrossRef]
26. Yang, Q.; Wang, Q.; Yu, Z. Substitution of alcohols by *N*-nucleophiles via transition metal-catalyzed dehydrogenation. *Chem. Soc. Rev.* **2015**, *44*, 2305–2329. [CrossRef]
27. Huang, F.; Liu, Z.; Yu, Z. C-Alkylation of Ketones and Related Compounds by Alcohols: Transition-Metal-Catalyzed Dehydrogenation. *Angew. Chem. Int. Ed.* **2016**, *55*, 862–875. [CrossRef]
28. Corma, A.; Navas, J.; Sabater, M.J. Advances in One-Pot Synthesis through Borrowing Hydrogen Catalysis. *Chem. Rev.* **2018**, *118*, 1410–1459. [CrossRef]
29. Alig, L.; Fritz, M.; Schneider, S. First-Row Transition Metal (De)Hydrogenation Catalysis Based on Functional Pincer Ligands. *Chem. Rev.* **2019**, *119*, 2681–2751. [CrossRef]
30. Irrgang, T.; Kempe, R. 3d-Metal Catalyzed *N*- and *C*-Alkylation Reactions via Borrowing Hydrogen or Hydrogen Autotransfer. *Chem. Rev.* **2019**, *119*, 2524–2549. [CrossRef]
31. Reed-Berendt, B.G.; Latham, D.E.; Dambatta, M.B.; Morrill, L.C. Borrowing Hydrogen for Organic Synthesis. *ACS Cent. Sci.* **2021**, *7*, 570–585. [CrossRef]
32. Volk, B.; Mezei, T.; Simig, G. Raney Nickel-Induced 3-Alkylation of Oxindole with Alcohols and Diols. *Synthesis* **2002**, *2002*, 595–597. [CrossRef]
33. Grigg, R.; Whitney, S.; Sridharan, V.; Keep, A.; Derrick, A. Iridium catalysed C-3 alkylation of oxindole with alcohols under solvent free thermal or microwave conditions. *Tetrahedron* **2009**, *65*, 4375–4383. [CrossRef]
34. Jensen, T.; Madsen, R. Ruthenium-Catalyzed Alkylation of Oxindole with Alcohols. *J. Org. Chem.* **2009**, *74*, 3990–3992. [CrossRef]
35. Bisht, G.S.; Chaudhari, M.B.; Gupte, V.S.; Gnanaprakasam, B. Ru-NHC Catalyzed Domino Reaction of Carbonyl Compounds and Alcohols: A Short Synthesis of Donaxaridine. *ACS Omega* **2017**, *2*, 8234–8252. [CrossRef]
36. Dambatta, M.B.; Polidano, K.; Northey, A.D.; Williams, J.M.J.; Morrill, L.C. Iron-Catalyzed Borrowing Hydrogen C-Alkylation of Oxindoles with Alcohols. *ChemSusChem* **2019**, *12*, 2345–2349. [CrossRef]
37. Saini, P.; Dolui, P.; Nair, A.; Verma, A.; Elias, A.J. A Bench-stable 8-Aminoquinoline Derived Phosphine-free Manganese (I)-Catalyst for Environmentally Benign C(alpha)-Alkylation of Oxindoles with Secondary and Primary Alcohols. *Chem. Asian J.* **2023**, *18*, e202201148. [CrossRef]
38. Wu, Q.; Pan, L.; Du, G.; Zhang, C.; Wang, D. Preparation of pyridyltriazole ruthenium complexes as effective catalysts for the selective alkylation and one-pot C–H hydroxylation of 2-oxindole with alcohols and mechanism exploration. *Org. Chem. Front.* **2018**, *5*, 2668–2675. [CrossRef]
39. Liu, G.; Huang, T.; Zhang, Y.; Liang, X.; Li, Y.; Li, H. C-3 alkylation of oxindole with alcohols catalyzed by an indene-functionalized mesoporous iridium catalyst. *Catal. Commun.* **2011**, *12*, 655–659. [CrossRef]
40. Chaudhari, C.; Siddiki, S.M.A.H.; Kon, K.; Tomita, A.; Tai, Y.; Shimizu, K. C-3 alkylation of oxindole with alcohols by Pt/CeO_2 catalyst in additive-free conditions. *Catal. Sci. Technol.* **2014**, *4*, 1064–1069. [CrossRef]
41. Putra, A.E.; Oe, Y.; Ohta, T. Pd/C-Catalyzed Alkylation of Heterocyclic Nucleophiles with Alcohols through the "Borrowing Hydrogen" Process. *Eur. J. Org. Chem.* **2015**, *2015*, 7799–7805. [CrossRef]
42. Fujita, S.; Imagawa, K.; Yamaguchi, S.; Yamasaki, J.; Yamazoe, S.; Mizugaki, T.; Mitsudome, T. A nickel phosphide nanoalloy catalyst for the C-3 alkylation of oxindoles with alcohols. *Sci. Rep.* **2021**, *11*, 10673. [CrossRef] [PubMed]
43. Li, J.; Yu, M.; Duan, Z.-C.; Zhu, H.; Yao, W.; Wang, D. Porous cross-linked polymer copper and iridium catalyzed the synthesis of quinoxalines and functionalized ketones under solvent-free conditions. *Mater. Chem. Front.* **2021**, *5*, 7861–7872. [CrossRef]
44. Zhao, S.; Wang, Y.; Dong, J.; He, C.-T.; Yin, H.; An, P.; Zhao, K.; Zhang, X.; Gao, C.; Zhang, L.; et al. Ultrathin metal–organic framework nanosheets for electrocatalytic oxygen evolution. *Nat. Energy* **2016**, *1*, 16184. [CrossRef]
45. Stoica, A.-C.; Damoc, M.; Zaltariov, M.-F.; Racles, C.; Cazacu, M. Two-dimensional coordination polymers containing permethylated motifs-promising candidates for 2D emerging materials. Structural, behavioral and functional particularities. *React. Funct. Polym.* **2021**, *168*, 105039. [CrossRef]
46. Farid, S.; Mao, Q.; Ren, S.; Hao, C.; Dong, X. Promoting the Oxygen Evolution Reaction via Morphological Manipulation of a Lamellar Nanorod-Assembled Ni(II)-Pyrazolate Superstructure. *ACS Appl. Mater. Interfaces* **2022**, *14*, 47775–47787. [CrossRef]
47. Duan, J.; Jin, W.; Kitagawa, S. Water-resistant porous coordination polymers for gas separation. *Coord. Chem. Rev.* **2017**, *332*, 48–74. [CrossRef]
48. Griffin, S.E.; Domecus, G.P.; Flores, C.E.; Sikma, R.E.; Benz, L.; Cohen, S.M. A Coordination Polymer of Vaska's Complex as a Heterogeneous Catalyst for the Reductive Formation of Enamines from Amides. *Angew. Chem. Int. Ed.* **2023**, *62*, e202301611. [CrossRef]

49. Gui, S.; Tang, W.; Huang, Z.; Wang, X.; Gui, S.; Gao, X.; Xiao, D.; Tao, L.; Jiang, Z.; Wang, X. Ultrasmall Coordination Polymer Nanodots Fe-Quer Nanozymes for Preventing and Delaying the Development and Progression of Diabetic Retinopathy. *Adv. Electron. Mater.* **2023**, 300261. [CrossRef]
50. Hu, X.; Zhu, H.; Sang, X.; Wang, D. Design and Synthesis of Zirconium-Containing Coordination Polymer Based on Unsymmetric Indolyl Dicarboxylic Acid and Catalytic Application on Borrowing Hydrogen Reaction. *Adv. Synth. Catal.* **2018**, *360*, 4293–4300. [CrossRef]
51. Sang, X.; Hu, X.; Tao, R.; Zhang, Y.; Zhu, H.; Wang, D. A Zirconium Indazole Carboxylate Coordination Polymer as an Efficient Catalyst for Dehydrogenation-Cyclization and Oxidative Coupling Reactions. *ChemPlusChem* **2020**, *85*, 123–129. [CrossRef]
52. Tao, R.; Yang, Y.; Zhu, H.; Hu, X.; Wang, D. Ligand-tuned cobalt-containing coordination polymers and applications in water. *Green Chem.* **2020**, *22*, 8452–8461. [CrossRef]
53. Chang, S.; Liu, H.; Shi, G.; Xia, X.-F.; Wang, D.; Duan, Z.-C. Copper–cobalt coordination polymers and catalytic applications on borrowing hydrogen reactions. *New J. Chem.* **2022**, *46*, 15929–15936. [CrossRef]
54. Han, M.-R.; Kong, X.-J.; Feng, S.-S.; Lu, L.-P. Synthesis, Structure and Magnetic Studies of a Ni(II) Coordination Polymer Constructed from Asymmetrical Tetracarboxylic Acid and N-Donor Ligand. *J. Clust. Sci.* **2021**, *33*, 809–814. [CrossRef]
55. Xu, J.; He, S.; Zhang, H.; Huang, J.; Lin, H.; Wang, X.; Long, J. Layered metal–organic framework/graphene nanoarchitectures for organic photosynthesis under visible light. *J. Mater. Chem. A* **2015**, *3*, 24261–24271. [CrossRef]
56. Osadchii, D.Y.; Olivos-Suarez, A.I.; Bavykina, A.V.; Gascon, J. Revisiting Nitrogen Species in Covalent Triazine Frameworks. *Langmuir* **2017**, *33*, 14278–14285. [CrossRef]
57. Jia, X.; Zhang, B.; Chen, C.; Fu, X.; Huang, Q. Immobilization of chitosan grafted carboxylic Zr-MOF to porous starch for sulfanilamide adsorption. *Carbohydr. Polym.* **2021**, *253*, 117305. [CrossRef]
58. Wu, H.; Li, S.; Liu, Y.; Liu, M.; Shi, Y. Metal–Organic Framework-Derived Hollow Carbon Nanosphere@Ni/Reduced Graphene Oxide Composites for Supercapacitor Electrodes with Enhanced Performance. *ACS Appl. Nano Mater.* **2023**, *6*, 1582–1591. [CrossRef]
59. Shang, X.F.; Morris-Natschke, S.L.; Yang, G.Z.; Liu, Y.Q.; Guo, X.; Xu, X.S.; Goto, M.; Li, J.C.; Zhang, J.Y.; Lee, K.H. Biologically active quinoline and quinazoline alkaloids part II. *Med. Res. Rev.* **2018**, *38*, 1614–1660. [CrossRef]
60. Juvale, K.; Gallus, J.; Wiese, M. Investigation of quinazolines as inhibitors of breast cancer resistance protein (ABCG2). *Bioorg. Med. Chem.* **2013**, *21*, 7858–7873. [CrossRef]
61. Michael, J.P. Quinoline, quinazoline and acridone alkaloids. *Nat. Prod. Rep.* **2002**, *19*, 742–760. [CrossRef] [PubMed]
62. Chen, Z.; Song, J.; Peng, X.; Xi, S.; Liu, J.; Zhou, W.; Li, R.; Ge, R.; Liu, C.; Xu, H.; et al. Iron Single Atom Catalyzed Quinoline Synthesis. *Adv. Mater.* **2021**, *33*, e2101382. [CrossRef] [PubMed]
63. Xu, X.; Ai, Y.; Wang, R.; Liu, L.; Yang, J.; Li, F. Ruthenium-catalyzed acceptorless dehydrogenative coupling of o-aminobenzyl alcohols with ketones to quinolines in the presence of carbonate salt. *J. Catal.* **2021**, *395*, 340–349. [CrossRef]
64. Yu, K.; Chen, Q.; Liu, W. Iron-catalysed quinoline synthesis via acceptorless dehydrogenative coupling. *Org. Chem. Front.* **2022**, *9*, 6573–6578. [CrossRef]
65. Hao, Z.; Zhou, X.; Ma, Z.; Zhang, C.; Han, Z.; Lin, J.; Lu, G.L. Dehydrogenative Synthesis of Quinolines and Quinazolines via Ligand-Free Cobalt-Catalyzed Cyclization of 2-Aminoaryl Alcohols with Ketones or Nitriles. *J. Org. Chem.* **2022**, *87*, 12596–12607. [CrossRef]
66. Chen, X.; Ai, Y.; Liu, D.; Liu, P.; Xu, X.; Yang, J.; Li, F. A recyclable covalent triazine framework-supported iridium(iii) terpyridine complex for the acceptorless dehydrogenative coupling of o-aminobenzyl alcohols with ketones to form quinolines. *Mater. Chem. Front.* **2022**, *6*, 1228–1235. [CrossRef]
67. Yang, L.; Wan, J.-P. Ethyl lactate-involved three-component dehydrogenative reactions: Biomass feedstock in diversity-oriented quinoline synthesis. *Green Chem.* **2020**, *22*, 3074–3078. [CrossRef]
68. Li, R.; Jiang, S.; Zheng, H.; Lei, H.; Huang, Z.; Chen, S.; Deng, G.-J. Iron-catalyzed indolo[2,3-c]quinoline synthesis from nitroarenes and benzylic alcohols/aldehydes promoted by elemental sulfur. *Green Synth. Catal.* **2022**, *3*, 95–101. [CrossRef]
69. Ghosh, A.; Bera, A.; Banerjee, D. Nickel Catalyzed Alkylation of Oxindoles with Alkyl Alcohols. *ChemCatChem* **2023**, *15*, e202201433. [CrossRef]
70. Jana, A.; Kumar, A.; Maji, B. Manganese catalyzed C-alkylation of methyl *N*-heteroarenes with primary alcohols. *Chem. Commun.* **2021**, *57*, 3026–3029. [CrossRef]